(23) Zhang, X. H.; West, R. *J. Polym. Sci.* **1984**, *22*, 159-170.
(24) Trefonas, P.; West, R.; Miller, R. D.; Hofer, D. *J. Polym. Sci., Polym. Lett. Ed.* **1983**, *21*, 828-829.
(25) Miller, R. D.; Hofer, D.; Wilson, C. G.; Trefonas, P.; West, R. *Polym. Prepr. (Am. Chem. Soc., Div. Polym. Chem.)* **1984**, *25*(1), 307-308.
(26) Stanislawski, D. A.; West, R. *J. Organometal. Chem.* **1981**, *204*, 307-314.
(27) Stanislawski, D. A.; West, R. *J. Organometal. Chem.* **1981**, *204*, 295-305.
(28) West, R.; Kramer, F. A.; Carberry, E. *J. Organometal. Chem.* **1967**, *8*, 79-85.
(29) Brough, L. F.; West, R. *J. Am. Chem. Soc.* **1981**, *103*, 3049-3056.
(30) Takeda, K.; Matsumoto, N. *Phys. Rev. B: Condens. Matter* **1984**, *30*, 5871-5876.
(31) Zeigler, J. M. *Polym. Prepr. (Am. Chem. Soc., Div. Polym. Chem.)* **1986**, *27*(1), 109-110.
(32) Berlman, I. B. *Handbook of Fluorescence Spectra of Organic Compounds*, 2nd ed.; Academic: New York, 1971.
(33) (a) Harrah, L. A.; Zeigler, J. M. *J. Polym. Sci., Polym. Lett. Ed.* **1985**, *23*, 209-211. (b) Schweizer, K. S. *Chem. Phys. Lett.* **1986**, *125*, 118-122. (c) Zeigler, J. M.; Adolf, D.; Harrah, L. A. Presented at the 20th Organosilicon Symposium, Tarrytown, NY, 1986; abstract P-2.25.
(34) Frank, C. W.; Harrah, L. A. *J. Chem. Phys.* **1974**, *61*, 1526-1541.
(35) Robin, M. B. *Higher Lying Excited States of Polyatomic Molecules*; Academic: New York, 1974; Vol. 1, pp 104-105.
(36) Dewar, M. J. S. *J. Am. Chem. Soc.* **1984**, *106*, 669-682.
(37) Klevens, H. B.; Platt, J. R. *J. Chem. Phys.* **1949**, *17*, 470-481.
(38) **Caution:** All solvents must be *thoroughly dry* and monomers pure to polymerize dihalosilanes safely. The use of wet solvents and/or impure monomers leads to dangerous induction periods in the polymerization reaction that can result in a violent and uncontrollable exotherm when polymerization finally initiates.
(39) Aleksandrova, Y. A.; Kotleva, N. S.; Sorokina, R. A.; Bakhurina, L. M.; Nikitina, T. S.; Panov, Y. M.; Pravednikov, A. N. *Vysokomol. Soyedin., Ser. A* **1969**, *11*, 2470.
(40) The curve shown in Figure 8 was normalized to pass through the highest molecular weight point in the asymptote.
(41) Loubriel, G.; Zeigler, J. M. *Phys. Rev. B: Condens. Matter* **1986**, *33*, 4203-4206.

Solid-State NMR Study of the Hexamethylenetetramine Curing of Phenolic Resins

Galen R. Hatfield and Gary E. Maciel*

Department of Chemistry, Colorado State University, Fort Collins, Colorado 80523.
Received August 19, 1986

ABSTRACT: The curing of a phenolic resin by hexamethylenetetramine (HMTA) is elucidated through the use of ^{13}C and ^{15}N CP/MAS NMR spectroscopy. The cure was shown to result in increased cross-linking, with the bridging carbons originating from the curing agent. Intermediates involved in the curing process are identified, with species having structures of the benzoxazine and tribenzylamine types being the major components. The results are compared to previous studies on model systems, and the power of solid-state NMR to probe chemistry in complex macromolecules is again clearly demonstrated.

Introduction

In 1907 a technique for processing phenol-formaldehyde resins, the first wholly synthetic commercial polymer material,[1] was developed by Baekeland. Today, phenolic resins have great commercial applications, especially as molding compounds, coatings, and industrial bonding resins. Details of the curing process are responsible for many of the important physical and mechanical characteristics of these materials. Thus, an explicit knowledge of the curing process is essential for understanding and improving the use of phenolic resins.

Although the curing of phenol-formaldehyde resins has received a great deal of attention,[1-12] most of the previous studies have suffered from experimental limitations, chiefly due to solubility limitations, dissolution uncertainties, and heavy reliance on model systems. Recent studies[13-16] have demonstrated the use of solid-state ^{13}C NMR with cross polarization (CP) and magic-angle spinning (MAS)[17-19] for systems warranting such concerns. The ^{13}C CP/MAS technique has proven to be a powerful tool for structural elucidation in macromolecular systems. It is the application of this technique to the investigation of the hexamethylenetetramine (HMTA) curing of a phenol-formaldehyde resin of the novolak type on which this paper focuses.

Experimental Section

NMR Measurements. ^{13}C CP/MAS spectra were obtained at 25.1 MHz on a home-built spectrometer that utilizes a Nicolet 1180 data system and a Nalorac 4.7-T magnet operated at half field. Spectra were obtained at numerous contact times, ranging from 0.5 to 4 ms, and the relative peak intensities showed no major dependence on contact time over that range. Spectra of the cured resins presented here were obtained with a 2-ms contact time and a 1-s repetition time. Samples were spun at 3.2-3.5 kHz, using spinners of the Windmill type.[20] The magic angle was adjusted to within 0.1° by using the ^{79}Br spectrum of KBr placed in a spinner.[21]

^{15}N CP/MAS spectra were obtained at 20.3 MHz on a modified wide-bore Nicolet NT-200 spectrometer. The NMR parameters used to accumulate the spectra presented here were a 4-ms contact time and a 15-s repetition time. Samples were spun at 2.2 kHz, using bullet-type spinners,[22] and the magic angle was again set by the KBr method.

Proton-decoupled solution-state ^{13}C spectra were obtained on an IBM WP-200SY spectrometer at a carbon frequency of 50.3 MHz, while ^{15}N solution-state spectra were obtained at 36.5 MHz on a Nicolet NT-360 spectrometer. All ^{13}C spectra were referenced externally to tetramethylsilane at 0 ppm and all ^{15}N spectra to liquid NH_3, also at 0 ppm.

Samples. The test resin used in this study was a novolak phenolic resin prepared at the Durez Division of the Occidental Chemical Corp. under conditions believed to produce a "random resin". The details of the ^{13}C CP/MAS spectrum of this resin have been reported previously.[13] The test resin was cured by heating a mixture of 90% resin plus 10% HMTA for 1 h at the temperature noted in the text. Both the ^{13}C- and ^{15}N-labeled HMTA used in this study were prepared by the method of Bulusu and co-workers,[23] using 99% ^{13}C-enriched CH_2O or 99% ^{15}N-enriched ammonium acetate, respectively.

Model compounds used in this study were either obtained commercially from Aldrich Chemical Co. or synthesized by using literature preparations, as noted in the text.

Results and Discussion

The key types of molecular structures that are known or suspected to be involved or of interest in this study are

* Author to whom correspondence should be addressed.

0024-9297/87/2220-0608$01.50/0

Table I
Structures and Key NMR Data on Proposed Intermediates (Parent Compounds)

prototype structure of proposed intermediate	structure	key ^{13}C chemical shift, ppm	key ^{15}N chemical shift, ppm
hexamethylenetetramine[a] (1)	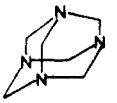	$-CH_2-$, 74.5	44
benzylamine (2)	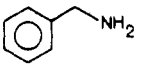	$-CH_2-$, 46.3[b]	24.6[c]
dibenzylamine (3)	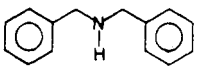	$-CH_2-$, 53.1[d]	41.6[c]
tribenzylamine (4)	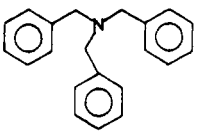	$-CH_2-$, 56.9[e]	51.8[f]
azomethine (5)	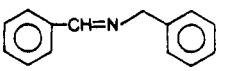	$-CH=$, 157–163[g]	318[h]
benzyl ether (6)	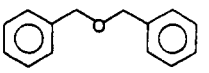	$-CH_2-$, 70[i]	
benzoxazine[j]	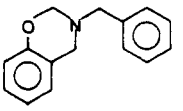	O–CH_2–N, 83[k] Ph–CH_2–N, 56, 52[k]	42.3[k]
hexiaminal (8)	NH_2CH_2OH	NH_2CH_2OH	
dimethylolamine (9)	$NH(CH_2OH)_2$	$NH(CH_2OH)_2$	
methylenediamine[l] (10)	$NH_2CH_2NH_2$	$NH_2CH_2NH_2$, 58.5[n] 48[n]	20.6[o]
1,3,5-hexahydro-*s*-triazine (11)		$-CH_2$, 61.6[p]	
1,5-endomethylene-1,3,5,7-tetrazacyclooctane (12)	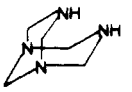	$-NH-CH_2-N$, 66.6[p] $N-CH_2-N$, 69.9[p]	
1,3,5-tribenzylhexahydrotriazine[q] (13)	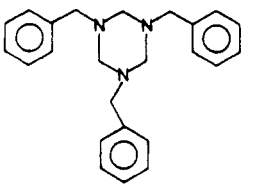	Ph–CH_2–N, 58[r] $N-CH_2-N$, 75[r]	49.8[r]
tetrabenzyldiaminomethane[s] (14)	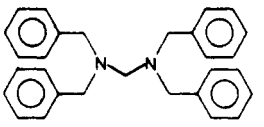	Ph–CH_2–N, 57[t] $N-CH_2-N$, 74[t]	51.0[t]
amide (15)	R-NH-CHO	160–180[u]	100–150[v]

[a] Prepared as in ref 23. [b] Taken from *The Sadtler Standard Carbon-13 NMR Spectra*; Sadtler Research Laboratories: Philadelphia, 1977; p 140. [c] Neat liquid. [d] *Sadtler*, p 1878. [e] *Sadtler*, p 224. [f] 2 g in 10 mL of diethyl ether. [g] Range given for aromatic imines, ref 42. [h] Value given for Ph—CH=N—DH_3, ref 38. [i] Values for various *o*-hydroxybenzyl ether isomers range from 69 to 72 ppm, ref 35. [j] Prepared as in: Weatherbee, C.; Law, H. K. S.; Snell, R.; Goken, G.; Van Lear, G. *Trans. Illinois State Acad. Sci.* **1963**, *56*, 12. [k] 4 g in 8 mL of acetone. [l] Unstable compound; see ref 29. [m] Predicted value from: Sarneski, J. E.; Suprenant, H. L.; Molen, F. K.; Reilley, C. N. *Anal. Chem.* **1975**, *47*, 2116. [n] Value taken for methylenediamine sulfate. [o] 5 g in 10 mL of 50% aqueous EtOH. [p] Value taken from: Nielsen, A. T.; Moore, D. W.; Ogan, M. D.; Atkins, R. L. *J. Org. Chem.* **1979**, *44*, 1678. [q] Prepared as in: McDonagh, A. F.; Smith, H. E. *J. Org. Chem.* **1968**, *33*, 8. [r] 3 g in 10 mL of MeOH. [s] Prepared as in: Weatherbee, C.; Law, H. K. S.; Snell, R.; Goken, G.; Van Lear, G. *Trans. Illinois State Acad. Sci.* **1963**, *56*, 12. [t] 1.5 g in 8 mL of acetone. [u] Range taken from ref 42. [v] Range taken from ref 38.

summarized in Table I along with their ^{13}C and/or ^{15}N chemical shifts. Boldface numbers in the text refer to these structures in Table I.

Hexamethylenetetramine (1), often called HMTA or HEXA, is the most common curing agent used in the manufacture of phenolic resins.[1] Despite years of study, the role of this key substance in the curing process has remained vague, at best. Previous studies in this laboratory[13] have shown that curing with HMTA results in increased cross-linking; however, details of the fate of HMTA during the curing process have, until now, been obscure.

Many intermediates in the curing process have been proposed,[1-12] and the parent compounds of each of these, as well as some others, are included in Table I. Those

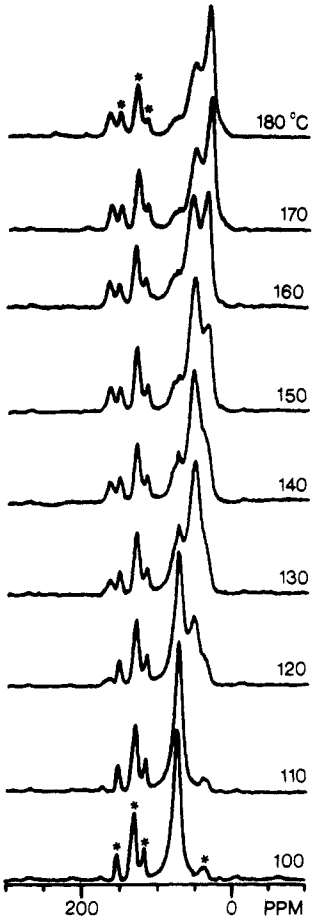

Figure 1. ^{13}C CP/MAS spectra of phenolic resin cured with ^{13}C-labeled HMTA for 1 h at the temperature indicated. Asterisks in the top and bottom spectra denote natural-abundance peaks.

receiving the most attention have been the substituted benzylamines (**2**–**4**). A thorough solution-state ^{13}C NMR study[12] of the reaction of phenol and HMTA revealed the presence of primary, secondary, and tertiary hydroxybenzylamines as reaction intermediates, strongly suggesting that the various substituted benzylamines are central to the curing mechanism of solid phenolic resins. Structures of the azomethine (**5**) type have also been proposed in an attempt to account for the deep yellow color of the cured resin. Benzyl ethers (**6**) and benzoxazines (**7**) have received less attention.

Some attention has been directed previously toward examining the sequential breakdown of HMTA as a possible clue to the curing mechanism. One can hope that insight into the breakdown mechanism can be gained from studying the formation of HMTA from NH_3 and CH_2O.[25-30] Although the exact details of the formation and breakdown mechanisms remain in question, most studies agree that intermediates of types **8**–**12** are involved. These compounds, as well as the benzyl-substituted analogues of the diamine (**13**) and triazine (**14**) were considered in the present study for completeness.

Although solid-state NMR studies of phenolic resins have been limited,[13,15,16] extensive ^{13}C NMR studies have been carried out in the solution state.[31-36] Peaks in the ^{13}C CP/MAS NMR spectra obtained in this study were assigned on the basis of comparison with peak assignments made in these earlier studies as well as with data on the model compounds and the proposed intermediates given in Table I. The details of the ^{13}C CP/MAS spectrum of the test resin and associated structural assignments have been reported previously[13] and will not be repeated here.

Table II
^{13}C NMR Liquid-State Assignments Based on Model Compounds

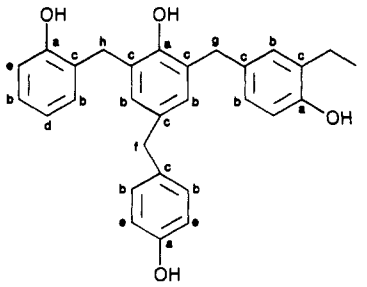

carbon	chemical shift, ppm	description[a]
a	150	hydroxy-substituted phenolic carbons
b	130	unsubstituted meta aromatic carbons
c	125	methylene-substituted aromatic carbons
d	120	unsubstituted para aromatic carbons
e	115	unsubstituted ortho aromatic carbons
f	40	para–para methylene bridge
g	35	ortho–para methylene bridge
h	30	ortho–ortho methylene bridge

[a] In these descriptions, ortho, meta, and para indicate the ring position relative to the OH group.

Shown in Figure 1 are the ^{13}C spectra obtained on a sample of the test resin after sequential heating for 1 h at each of several discrete temperatures, ranging from 100 to 180 °C, with ^{13}C-labeled HMTA. Each spectrum in Figure 1 is plotted such that the intensity of the peak at 152 ppm remains constant throughout the figure. This peak, as can be seen from Table II, is due to OH-substituted carbons of phenolic moieties and as such should remain relatively constant throughout the curing process. Other resonances at 132, 117, and 35 ppm have also been assigned to various carbon environments in the resin.[13]

It can be seen from Figure 1 that as the curing temperature is increased several prominent changes occur in the intensity distribution. At the lower temperatures (100–120 °C), the dominant ^{13}C peak is at 75 ppm and can be assigned to HMTA. As the temperature is increased this peak gradually decreases in relative intensity and another peak, located at 55 ppm, begins to dominate the spectra. The peak is initially observed at 120 °C, becomes the most prominent peak by 130 °C, and gradually decreases thereafter with increasing curing temperature. Also note that, concurrent with the appearance of the peak at 55 ppm, a shoulder appears at 83 ppm; however, the relative intensity of the 83 ppm shoulder appears to decrease more dramatically with increasing temperature than does the 55 ppm peak. The relative intensities of these peaks are overshadowed at higher temperatures by a third region, at 33 ppm, which dominates the spectra at 160–180 °C. The intensity around 33 ppm can be assigned to the various methylene bridges that occur upon cross-linking (e.g., h, g, f, in Table II) and originate from the HMTA initially present. Note that in the spectra for the lower curing temperatures (100–110 °C) this peak is present in natural-abundance intensity, but as the curing process progresses, the dramatic increase in intensity could arise only from the addition of ^{13}C-labeled methylene carbons.

Figure 1 thus reveals some very important facts. The first, established previously,[13] is the fact that curing results in increased methylene cross-linking. The second fact is that these methylene bridges originate from the methylene carbons of HMTA. To the best of our knowledge, this is the first physical proof of the reasonable assumption that the carbons of HMTA eventually become methylene

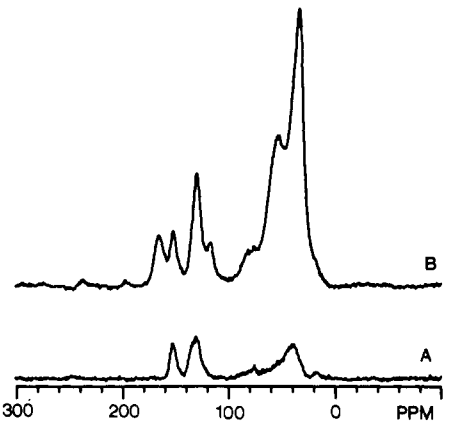

Figure 2. ^{13}C CP/MAS spectra of resin cured with ^{13}C-labeled HMTA at 180 °C: (A) interrupted decoupling with 50-μs delay; (B) normal spectrum (no delay).

bridges in the resin and are therefore responsible for the observed increase in cross-linking. Also, the observed intensity at 83 and 56 ppm reveals the presence of at least one intermediate formed from HMTA during the cure. The intensity behavior of these two peaks suggests that they represent the major intermediate(s) in the curing process. Another peak, at 167 ppm, appears during the cure at 120 °C and remains essentially constant after 150 °C. The identity of this curing byproduct will be discussed later.

To aid in identifying the structures responsible for the peaks at 55, 83, 33, and 167 ppm, dipolar-dephasing (interrupted decoupling)[37] experiments were carried out on the test resin cured with ^{13}C-labeled HMTA. In these experiments, a delay period of 50 μs is inserted between the CP contact period and data acquisition, during which the ^{1}H decoupler is turned off and ^{13}C magnetization due to ^{13}C's that have strong dipolar interactions with protons is attenuated by dipolar dephasing. In the resulting spectrum, intensities from methyl and nonprotonated carbons strongly persist, while intensities from methylene and methine carbons is diminished. Results from the interrupted-decoupling experiment applied to the resin cured at 180 °C are given in Figure 2A. Note that the intensity in all the regions of interest is diminished relative to that of the normal CP/MAS experiment (Figure 2B). Intensity from the methylene carbons of HMTA (75 ppm) and the bridging CH_2 carbons (33 ppm) is reduced, as expected. Intensities of the unassigned peaks at 167, 83, and 55 ppm are also dramatically reduced in Figure 2A, revealing that they arise from carbon moieties with one or two hydrogens directly attached to carbon. The C–OH peak at 152 ppm in Figure 2A is only slightly attenuated, as expected.

Examination of Table I reveals that all of the proposed intermediates contain CH_2 or CH groups; however, by considering the observed chemical shifts, one can eliminate some of them from further consideration in the assignment of the peaks at 83 and 55 ppm. Consideration of the 167 ppm peak is deferred. The transition of tribenzylamines (**4**) to dibenzylamines (**3**) to benzylamines (**2**), which has been observed in the solution state,[12] seems an unlikely explanation for the patterns shown in Figure 1, since it would not account for intensity at 83 ppm and since no intensity at 46 ppm due to CH_2 groups of benzylamines (**2**) is observed in Figure 1. Benzyl ethers (**6**), 1,3,5-hexahydro-*s*-triazine (**11**) and 1,5-endomethylene-1,3,5,7-tetrazycyclooctane (**12**) all have carbons that would yield ^{13}C resonances in regions distinctly different from what is observed in Figure 1. Note, however, that the benzoxazine structure (**7**) contains carbons that would account for intensity at both 83 and 55 ppm, strongly suggesting that benzoxazines are involved in the curing process. This possibilty is verified below. If structures of the benzoxazine type were the only HMTA-derived intermediates present in the curing process, the intensity ratio of peaks at 83 and 55 ppm would be 1:2. Intensity at 55 ppm is much higher in Figure 1 than this ratio would dictate, indicating the presence of another intermediate in the curing process. Note also from Table I that the methylene carbons of a tribenzylamine (**4**) system appear at 56 ppm and could account for the extra intensity observed in this region; however, a similar statement could also be made for the benzyl-substituted triazines (**13**) and diamines (**14**).

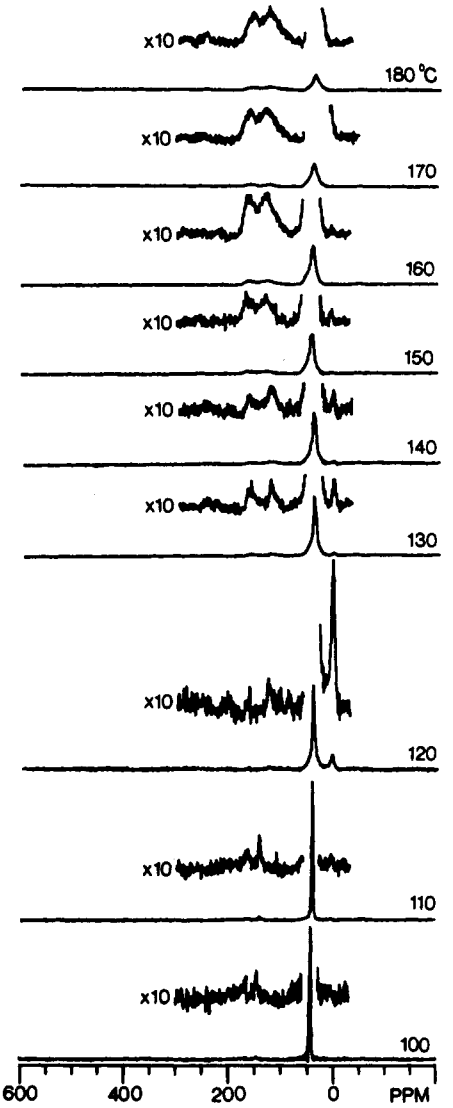

Figure 3. ^{15}N CP/MAS spectra of phenolic resin cured with ^{15}N-labeled HMTA for 1 h at the temperature indicated.

To aid in elucidating details of the curing process, ^{15}N CP/MAS spectra were obtained on the same test resin cured over the 100–180 °C temperature range with ^{15}N-labeled HMTA. The spectra obtained are given in Figures 3–6. The ^{15}N CP/MAS spectra taken as a function of the cure temperature over the 100–180 °C range are shown in Figure 3. The changes that are seen in the ^{15}N spectra are far less dramatic than those observed in the analogous ^{13}C series of Figure 1. Note that as the curing temperature is increased, the peak at about 40 ppm gradually broadens and decreases in intensity. It can also be seen from the expansions in Figure 3 that some intensity at 154 ppm also appears as the curing temperature is increased. Careful

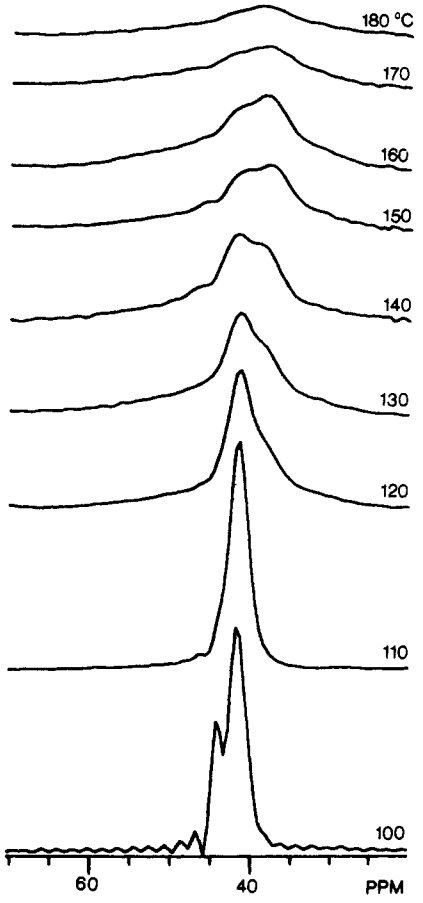

Figure 4. Expansions of spectra in Figure 3.

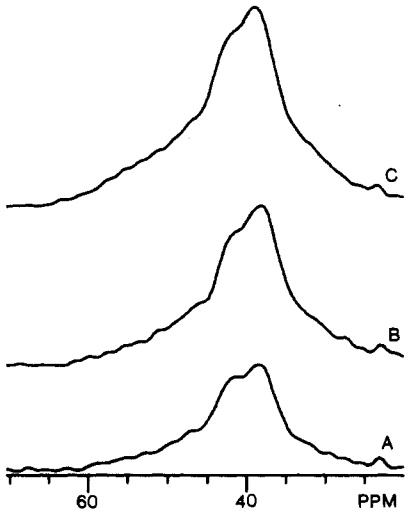

Figure 5. ^{15}N CP/MAS spectra of resin cured with ^{15}N-labeled HMTA to 180 °C: (A) interrupted decoupling with 125-μs delay; (B) 50-μs delay; (C) normal spectrum (no delay).

examination of this region in the ^{15}N spectrum shows that this resonance appears at 110 °C and gradually but steadily increases as the temperature is increased beyond 110 °C. Assignment of this resonance will be treated later. Intensity just to the right of this peak is due to a spinning sideband and can be seen to change in position from one curing temperature to another with slight differences in spinning speed. One can also see the appearance of an intense peak at 3 ppm in the spectrum of the sample heated at 120 °C. The intensity of this peak is markedly reduced by 130 °C curing and cannot be detected in samples cured at temperatures higher than 150 °C. This peak is readily assigned to NH_3, which initially becomes trapped

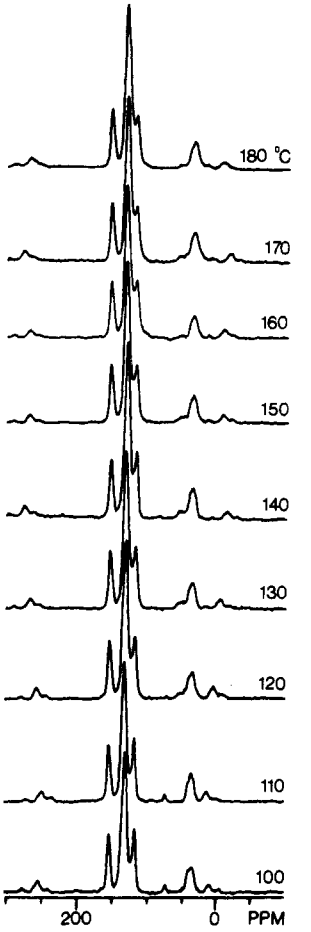

Figure 6. ^{13}C CP/MAS spectra of resin cured with ^{15}N-labeled HMTA for 1 h at the temperature indicated.

in the resin upon curing and is released at higher temperatures. The generation and evolution of NH_3 has long been observed to occur during the HMTA curing of phenolic resins and represents the ultimate fate of HMTA.[1,2,5,11]

The intensity around 40 ppm in the spectra of Figure 3 actually contains a considerable degree of structure, as seen in the expansion of this spectral region shown in Figure 4. One can see from the expansions that, at the outset of cure, intensity around 40 ppm is actually split into peaks at 44 and 41 ppm. Following the initial curing period at 100 °C, the intensity at 44 ppm disappears. Gradually, the intensity of the peak at 41 ppm decreases as the curing temperature is increased, while a shoulder at 38 ppm in turn increases. As the curing temperature is increased above 120 °C, the ^{15}N resonance pattern broadens and perhaps incorporates contributions from other isotropic chemical shifts (e.g., 55 and 37 ppm).

An interrupted-decoupling ^{15}N experiment was carried out on the resin cured at 180 °C, and the results are given in Figure 5. Intensity at 154 ppm (not shown in Figure 5) was found to disappear on interrupted decoupling, while most of the intensity from 50 to 38 ppm was found to persist, even after an interrupted-decoupling period as long as 125 μs. This experiment was also repeated at −70 °C (not shown) with a vacuum-dried sample to reduce the likelihood that H_2O-induced proton exchange was responsible for the interrupted-decoupling result obtained at room temperature. At the lower temperature, intensity was still found to persist thoughout the region from 50 to 38 ppm. Thus, the ^{15}N resonances from 50 to 38 ppm *cannot* be due to nitrogens with either one or two directly

attached protons. This is a pivotal result in identification of the curing intermediates. None of the direct breakdown products of HMTA (8–12) can now be considered further because they all contain –NH– or $-NH_2$ groups, which would show rapid dipolar dephasing. Structures of the azomethine (5) type can also be eliminated, since no intensity in the ^{15}N spectra appears at a shielding lower than 300 ppm. In addition, on the basis of the dipolar-dephasing results, the transition of tribenzylamines (4) to dibenzylamines (3) to benzylamines (2), observed in the solution state,[13] can also be discounted due to the presence of –NH– and $-NH_2$ moieties in these structures. Thus, through a combination of ^{13}C and ^{15}N NMR, including dipolar-dephasing experiments, many of the intermediates considered above, including models of curing determined from solution-state studies, must be eliminated from further consideration in the curing mechanism for the solid resin, and a new model of curing as it occurs in the solid state must be proposed.

One apparent anomaly in the results presented here so far warrants explicit mention at this point. Note that in Figure 1, ^{13}C intensity corresonding to HMTA (75 ppm) gradually decreases over a wide temperature range. However, in Figure 4 the ^{15}N intensity corresponding to HMTA (44 ppm) disappears essentially completely in the 110 °C curing. In order to determine whether the ^{13}C- and ^{15}N-labeled HMTA samples were for some anomalous reason (say, impurities) causing different curing rates and behaviors, ^{13}C CP/MAS spectra were also obtained on the ^{15}N-enriched cured resin samples for which ^{15}N spectra were given in Figure 4. Figure 6 shows these natural-abundance ^{13}C CP/MAS results obtained for the resin cured with ^{15}N-labeled HMTA. Although the ^{13}C spectral changes observed in Figure 6 are not as obvious as those in Figure 1, the ^{13}C intensity changes that occur in both sets of experiments closely agree with each other. ^{13}C NMR intensity due to HMTA gradually decreases with increasing cure temperature in Figure 6, as it does in Figure 1. Other spectral changes, such as the growth and subsequent loss of intensity around 55 ppm as well as the growth in intensity at 35 ppm, are seen to correspond for Figures 1 and 6. This reveals, as expected, that the curing process occurred with the same temperature dependence for both the sample cured with ^{13}C-enriched HMTA and the sample cured with ^{15}N-enriched HMTA. Therefore, the apparent anomaly noted above simply means that certain changes that are occurring during the cure are observable in the ^{15}N NMR experiment but not in the ^{13}C NMR experiment.

Solid Resin Cure. Through the use of the ^{13}C and ^{15}N CP/MAS NMR results, it is possible to trace the fate of HMTA and its successor molecules throughout the curing process. Tables I–III summarize the chemical shift data used to identify the curing intermediates. Table III also contains some previously unreported ^{15}N chemical shifts encountered in this project but not specifically relevant to the discussion below.

HMTA, in its original crystalline state, is observed at 75 ppm in the ^{13}C experiment and at 44 ppm in the ^{15}N experiment. Upon heating, the crystalline HMTA becomes incorporated into the phenolic resin matrix, losing its crystallinity and becoming involved in hydrogen bonding with phenolic OH groups and/or occluded H_2O. This change is observed by the immediate shift in intensity in the ^{15}N NMR spectrum from 44 to 41 ppm (Figure 4), and since such a change in the nature of HMTA is not observed in the ^{13}C experiment, this behavior accounts for the anomaly in temperature effects discussed above. HMTA,

Table III
Solvent and State Effects on Relevant ^{15}N Chemical Shifts[a]

compound	condition	^{15}N, ppm
HMTA (1)	solid	44.0
	0.5 g in 10 mL of H_2O	44.0
	0.5 g in 10 mL of *m*-cresol	42.0
benzylamine (2)	neat	24.6
	1:1 in *m*-cresol	28.9
benzylamine HCl	solid	49.0
dibenzylamine (3)	neat	41.6
	1:1 in *m*-cresol	48.5
2,2′-dihydroxydibenzylamine[b]	2 g in 8 mL of ethanol	38.0
tribenzylamine (4)	solid[c]	51.0
	2 g in 10 mL of ether	51.8
	1 g in 10 mL of *m*-cresol	51.7
	10% incorporation into polystyrene swelled with $CDCl_3$	35–60
tribenzylamine HCl	solid	61.0
benzoxazine (7)	4 g in 8 mL of acetone	42.3
	4 g in 8 mL of *m*-cresol	42.7
1,3,5-tribenzylhexahydrotriazine (13)	3 g in 10 mL of MeOH	49.8
tetrabenzyldiaminomethane (14)	1.5 g in 8 mL of acetone	50.6
	1.5 g in 8 mL of *m*-cresol	50.7

[a] All reported results determined in this study. [b] Prepared as in ref 2. [c] Prepared as in: Mason, A. T. *J. Chem. Soc.* **1893**, *63*, 1311.

dissolved in *m*-cresol, yields a ^{15}N chemical shift of 42 ppm. ^{15}N chemical shifts of amines typically move to lower shielding upon formation of a hydrogen bond;[38-40] however, HMTA has previously been shown to be an anomaly in this respect,[41] and this behavior is confirmed by the results given here for a *m*-cresol solution. A solution of HMTA in *m*-cresol yielded a ^{13}C NMR spectrum with a HMTA chemical shift within 0.7 ppm of its solid-state value, indicating that the hydrogen-bonding change in the chemical nature of HMTA is directly observable in the ^{15}N NMR experiment but is not so easily observed via ^{13}C NMR.

Once the HMTA is incorporated into the resin matrix, its rings open as it reacts with the resin to form a variety of intermediates. These intermediates may appear either simultaneously or sequentially during the cure. A more exhaustive and quantitative study designed to yield exact NMR intensity ratios might make it possible to choose between the various possible mechanistic routes. Even without such a study, it is reasonable to make useful inferences based on more qualitative spectral changes. For example, in terms of growth and disappearance, the ^{13}C NMR peaks at 83 and 56 ppm in Figure 1 are strongly correlated. This behavior, in view of the data summarized in Table I, indicates the presence of structures of the benzoxazine (7) type throughout the cure. This type of structure, along with hydrogen-bound HMTA, also accounts for the ^{15}N NMR intensity shown at 41 ppm in Figure 4.

In Figure 6, one can note that the intensity due to HMTA (75 ppm) is no longer observable when the curing temperature reaches 130 °C. While it is possible that some HMTA persists into the higher curing temperatures (undetected because of unfavorable CP dynamics, e.g., reflecting altered molecular motion), it seems unlikely that it would constitute a significant fraction of the 75 ppm ^{13}C intensity shown in the higher temperature regions of Figure 1. At the higher temperatures, intensity at 75 ppm in Figure 1 most likely contains contributions from structures of the benzyl-substituted triazine (13) and benzyl-substituted diamine (14) types. These structures also contribute to intensity around 57 ppm in the ^{13}C experiment.

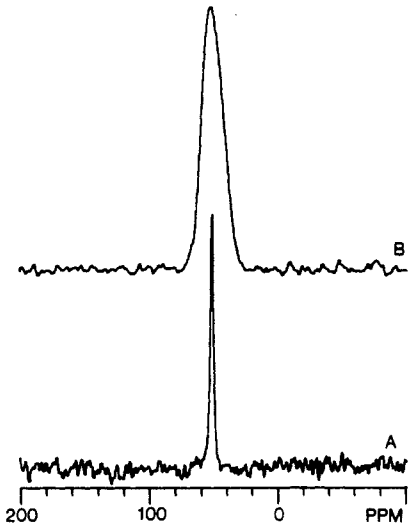

Figure 7. ^{15}N CP/MAS spectra of tribenzylamine: (A) crystalline; (B) 10% incorporated into $CDCl_3$-swelled polystyrene, excess $CDCl_3$ removed under vacuum.

From Table I we can see that structures of the benzyl-substituted triazine (**13**) and diamine (**14**) types give rise to ^{15}N intensity in the region of 50 ppm. Examination of Figure 4 reveals a broad shoulder of intensity from 47 to 53 ppm that appears upon curing at 140 °C. Thus, both the ^{13}C and ^{15}N spectra indicate the presence of benzyl-substituted triazines (**13**) and diamines (**14**) during the curing process.

While benzyl-substituted triazines (**13**) and diamines (**14**) are almost certainly present during the cure, they alone could not account for all of the ^{13}C intensity observed around 56 ppm in Figure 1. At most, the ratio of intensities of peaks at 75 and 55 ppm could be 1:4 if only structure **14** were present. However, this ratio is as low as roughly 1:15 for the resin cured at 180 °C. Thus, another type of intermediate must predominate. The tribenzylamine-type structure (**4**), which gives rise to ^{13}C NMR intensity at only 56 ppm in the methylene region, could certainly account for this pattern.

Although the dominance of tribenzylamine (**4**) structures is clear from the ^{13}C results, a correspondingly large region of intensity around 52 ppm in the ^{15}N experiment is not as obvious. As mentioned above, and as seen in Tables I and III, the ^{15}N chemical shift for some species is extremely sensitive to the geometrical environment of the ^{15}N nucleus. Hence, the possibility that the tribenzylamine ^{15}N peak has been shifted substantially away from 52 ppm by matrix-induced geometrical perturbations in the resin matrix is of interest. This was explored by introducing tribenzylamine into a polymer matrix. When tribenzylamine is introduced into $CDCl_3$-swelled polystyrene, the line width of its ^{15}N CP/MAS resonance increases from about 30 Hz to roughly 300 Hz. This result, which we believe reflects the structural properties of tribenzylamine in the crystalline and amorphous states, is shown in Figure 7. The observed increase in ^{15}N line width reflects the wide variety of C–N–C bond angles assumed by the benzyl groups surrounding the nitrogen atom in the milieu of an amorphous polymer. This, together with hydrogen bonding and Bronsted acid–base involvement of the phenolic OH groups, is the kind of disordered environment one might expect within the matrix of the phenolic resin. In order to prove that the 300-Hz line width of Figure 7B is due to chemical-shift dispersion and not some kind of intrinsic relaxation (T_2) mechanism, a Hahn spin echo experiment was carried out on the broad-line sample corresponding to Figure 7B. The natural ^{15}N line width determined in this manner is 76 Hz, showing that the total line width observed is largely due to chemical-shift dispersion, i.e., due to structural heterogeneity. A solution-state ^{15}N NMR spectrum of the tribenzylamine/polystyrene sample dissolved in $CDCl_3$ (not shown) contained a single sharp line at 52 ppm, proving that the spectrum obtained in Figure 7B is due to tribenzylamine and that no chemical reaction had occurred upon introduction of the tribenzylamine into the swelled polystyrene.

Careful examination of Figure 4 reveals the presence of a large, broad "foot" of intensity observable in the spectrum for each curing temperature above 110 °C. This foot is even more clearly seen in the enlarged spectra given in Figure 5. This broad component in the ^{15}N spectrum is assigned to tribenzylamine-type structures and corresponds to ^{13}C intensity at 56 ppm (Figure 1). Thus, the dominance of this species in the curing process can be demonstrated in both the ^{13}C and ^{15}N results.

^{15}N NMR intensity at 38 ppm, observed as a shoulder in the spectra of Figure 4 for samples cured at temperatures from 120 to 180 °C, is assignable to the ammonium ion, which can be seen in Table III to manifest this ^{15}N chemical shift. In order to verify that this resonance was due to the NH_4^+ ion in these samples, a single-pulse FT ^{15}N NMR experiment (spectrum not shown) was also carried out on the resin. This experiment, completely analogous to that done in the solution state except for the high-power ^1H decoupling employed in the present case, will discriminate against those entities that are rigid and will allow the observation of only highly mobile species. Application of the single-pulse FT experiment to the cured resin revealed a sharp line at 38 ppm, confirming that the highly mobile NH_4^+ ion is present in the cured resin, a conclusion that is entirely reasonable in light of the repeated observations of ammonia evolved during the cure.[1,2,5,11]

In addition to the generation of methylene linkages during the cure, as discussed above, a side reaction in the curing process can be seen in the appearance of ^{13}C intensity at 167 ppm (Figures 1 and 6) and ^{15}N intensity at 154 ppm (Figure 3). Intensities in these regions appear in the spectra of the resins cured at 110 and 120 °C, maximize in the spectrum of the resin cured at 150 °C, and remain relatively constant for higher curing temperatures. These resonances can be assigned to amide-type functionalities.[38,42] As mentioned above, both the ^{13}C intensity at 167 ppm (Figure 1) and the ^{15}N intensity at 154 ppm (Figure 3) disappeared in the interrupted-decoupling experiment. This indicates the presence of either one or two hydrogen atoms attached to each of the carbon and nitrogen atoms of these moieties. Hence, these amide moieties must have structures of the type R–NH–CHO.

Comparison with Solution-State Results. The most striking difference between our results and those of solution-state model studies is the absence of appreciable concentration of intermediates of the benzylamine, dibenzylamine, and azomethine (**5**) types in the solid-state case. No evidence whatsoever was found that would indicate the presence of azomethine (**5**) structures in the solid-state case. Benzylamine and dibenzylamine structures were discounted on the basis on the ^{15}N interrupted-decoupling results. With the exception of the minor formamide-type byproduct, no evidence could be found in this work for any intermediate containing either –NH– or $-NH_2$ (in particular dibenzylamine-type and benzylamine-type) functionalities. The ultimate fate for most of the nitrogen atoms originating from HMTA is evolution

as ammonia gas; some nitrogen persists in the form of the tertiary nitrogen functionalities discussed above. It seems plausible that the transformation steps from structures of the tribenzylamine (4) type to ammonia include steps that involve analogous dibenzylamine (3) and benzylamine (2) structures. However, if this is the case, then these intermediates (2 and 3) must be more reactive to further transformation than is their precursor (4), resulting in a "cascade" type of process that does not permit the direct observation of those intermediates. Intermediates containing dibenzylamine and benzylamine functionalities might react more slowly in solution. The observation in the present study of benzyl-substituted triazines (13) and diamines (14), which were not observed in solution-state model studies,[2,12] most likely can be attributed to the complexity of the resin matrix, as opposed to the relative simplicity of model systems.

Conclusions

Through the combination of ^{13}C and ^{15}N CP/MAS NMR studies, the intermediates in the curing of phenolic resins by HMTA have been identified. The two major successor molecules to HMTA are structures of the benzoxazine (7) and tribenzylamine (4) types. The methylene carbons of the curing agent have been shown to provide the increased methylene bridging involved in the cross-linking responsible for the resin cure. The results obtained in this study of curing in the solid resin are different from those reported earlier on model systems, although they may provide complementary information. This study again demonstrates both the power and the role of solid-state NMR for the characterization of solid complex macromolecules, especially when more than one nuclide can be employed.

Acknowledgment. We acknowledge financial support of this work by grants from the U.S. Department of Agriculture and the National Science Foundation (Grant No. DMR-8418446) and use of the Colorado State University Regional NMR Center funded by National Science Foundation Grant CHE-8208821. We also gratefully acknowledge Dr. Stanley Sojka and Occidental Chemical Co. for providing phenolic resins and the late Richard Bryson for providing much of the initial inspiration for this study.

Registry No. 1, 100-97-0; $(C_6H_5OH)(HCHO)$ (copolymer), 9003-35-4.

References and Notes

(1) Knop, A.; Scheib, W. *Chemistry and Application of Phenolic Resins*; Springer-Verlag: New York, 1979.
(2) Kopf, P. W.; Wagner, E. R. *J. Polym. Sci., Polym. Chem. Ed.* **1973**, *11*, 939.
(3) Megson, N. J. L. *Phenolic Resin Chemistry*; Butterworth: London, 1958.
(4) Martin, R. W. *Chemistry of Phenolic Resins*; Wiley: New York, 1956.
(5) Orrell, E. W.; Burns, R. *Plast. Polym.* **1968**, *36*(Oct), 469.
(6) Pshenitsyna, V. P.; Kotrolev, M. V. *Vysokomol. Soedin., Ser. A* **1969**, *1*, 733.
(7) Kurachenkov, V. I.; Igonin, L. A. *J. Polym. Sci., Polym. Chem. Ed.* **1971**, *9*, 2283.
(8) Zinke, A.; Zigeuner, G.; Weiss, G.; Wiesenberger, E. *Monatsh. Chem.* **1949**, *80*, 160.
(9) Ziquener, G.; Weishsel, H. *Monatsh. Chem.* **1955**, *86*, 858.
(10) *Kirk-Othmer Encycl. Chem. Technol., 2nd Ed.*; **1968**, *15*, 188.
(11) *Encycl. Polym. Sci. Technol.* **1969**, *10*, 27.
(12) Sojka, S. A.; Wolfe, R. A.; Guenther, G. D. *Macromolecules* **1981**, *14*, 1539.
(13) Bryson, R. L.; Hatfield, G. R.; Early, T. A.; Palmer, A. R.; Maciel, G. E. *Macromolecules* **1983**, *16*, 1669.
(14) Maciel, G. E.; Chuang, I.-S.; Gollob, L. *Macromolecules* **1984**, *17*, 1081.
(15) Fyfe, C. A.; McKinnon, M. S.; Rudin, A.; Tchir, W. J. *Macromolecules* **1983**, *16*, 1216.
(16) Fyfe, C. A.; Rudin, A.; Tchir, W. *Macromolecules* **1980**, *13*, 1322.
(17) Schaefer, J.; Stejskal, E. O. *J. Am. Chem. Soc.* **1976**, *98*, 1031.
(18) Pines, A.; Gibby, M. G.; Waugh, J. S. *J. Chem. Phys.* **1973**, *59*, 569.
(19) Schaefer, J.; Stejskal, E. O. *Topics in Carbon-13 NMR Spectroscopy*; Levy, G. C., Ed.; Wiley: New York, 1979; Vol. I.
(20) Wind, R. A.; Anthonio, F. E.; Duijvestijn, M. J.; Smidt, J.; Trommel, J.; deVette, G. M. C. *J. Magn. Reson.* **1983**, *52*, 424.
(21) Frye, J. S.; Maciel, G. E. *J. Magn. Reson.* **1982**, *48*, 125.
(22) Bartuska, V. J.; Maciel, G. E. *J. Magn. Reson.* **1981**, *42*, 312.
(23) Bulusu, S.; Autera, J.; Axenrod, T. *J. Labelled Compd. Radiopharm.* **1980**, *17*, 707.
(24) Ogata, Y.; Kawasaki, A. *Bull. Chem. Soc. Jpn.* **1964**, *37*, 514.
(25) Nielsen, A. T.; Moore, D. W.; Ogan, M. D.; Atkins, R. L. *J. Org. Chem.* **1979**, *44*, 1678.
(26) Bose, S. *J. Indian Chem. Soc.* **1957**, *34*, 663.
(27) Baur, E.; Roetschi, W. *Helv. Chim. Acta* **1941**, *24*, 754.
(28) Richmond, H. H.; Myers, G. S.; Wright, G. F. *J. Am. Chem. Soc.* **1949**, *70*, 3659.
(29) Duden, D.; Scharf, M. *Liebigs Ann. Chem.* **1985**, *288*, 218.
(30) Ogata, Y., Kawasaki, A. *The Chemistry of the Carbonyl Group*; *Zabicky*, J., Ed.; Interscience: London, 1970; Vol. II.
(31) Dradi, E.; Casirachi, G.; Casnati, G. *Chem. Ind. (London)* **1978**, Aug 19, 627.
(32) Siling, M. E.; Urman, Y. G.; Adorova, I. V.; Alekseyeva, S. G.; Matyukhina, O. S.; Slonim, I. Y. *J. Polym. Sci.* **1977**, 358.
(33) Sojka, S. A.; Wolfe, R. A.; Deitz, E. A.; Dannels, B. F. *Macromolecules* **1979**, *12*, 767.
(34) Kim, M. G.; Tiedeman, G. T.; Amons, L. W. *Weyerhaeuser Sci. Symp.* **1981**, *2*.
(35) deBreet, A. J. J.; Dankelman, W.; Huysmans, G. B.; deWit, J. *Angew. Makromol. Chem.* **1977**, *62*, 7.
(36) Mukoyama, Y.; Tanno, T.; Yokokawa, H.; Fleming, J. *J. Polym. Sci., Polym. Chem. Ed.* **1973**, *2*, 3193.
(37) Opella, S. J.; Frey, M. P. H. *J. Am. Chem. Soc.* **1979**, *101*, 5854.
(38) Levy, G. C.; Lichter, R. L. *Nitrogen-15 Nuclear Magnetic Resonance Spectroscopy*; Wiley-Interscience: New York, 1979.
(39) Paolillo, L.; Becker, E. D. *J. Magn. Reson.* **1970**, *2*, 168.
(40) Lichter, R. L.; Roberts, J. D. *J. Am. Chem. Soc.* **1972**, *94*, 2495.
(41) Cralk, D. J.; Levy, G. C.; Lombardo, A. *J. Phys. Chem.* **1982**, *86*, 3893.
(42) Levy, G. C.; Lichter, R. L.; Nelson, G. L. *Carbon-13 Nuclear Magnetic Resonance Spectroscopy*; Wiley-Interscience: New York, 1980.